J Nanostruct 15(1): 229-238, Winter 2025

RESEARCH PAPER

Structural and Optical Properties of Mn_3O_4:NiO Nanostructure Thin Films Prepared by Chemical Spray Pyrolysis Method

Ali Y. Ibrahim *, Faisal G. Hammoodi

Department of Physics, College of Science, University of Diyala, Iraq

ARTICLE INFO

Article History:
Received 07 October 2024
Accepted 22 December 2024
Published 01 January 2025

Keywords:
AFM
Mn_3O_4
NiO
Optical Properties
Thin Films
XRD

ABSTRACT

Thin films of pure manganese oxide doped with nickel oxide in ratios (0, 1 , 3 , 5 , 7) % were successfully prepared by chemical spray pyrolysis method. The films were deposited on glass slides at a temperature of 350 °C. The thin films were tested by using X-ray diffraction (XRD). According to the findings, the produced films possessed a polycrystalline quaternary structure . and all the films Visual tests were also carried out using (UV–Visible). We notice that the transmittance of the prepared films increases with increasing doping rates, and its best value is at 3%, but the absorbance will decrease because the behavior of absorbance is opposite to transmittance. The absorption coefficient, refractive index , and energy gap will increase with the increase in photon energy, as we notice that the energy gap values range between (2.65 – 2.95) eV.The extinction coefficient will decrease with increasing photon energy . A study was topographic on the surface of thin films using (AFM) and we notice that the roughness values of the thin films will decrease and the root mean square will also decrease.

How to cite this article
Ibrahim A., Hammoodi F. Structural and Optical Properties of Mn_3O_4:NiO Nanostructure Thin Films Prepared by Chemical Spray Pyrolysis Method. J Nanostruct, 2025; 15(1):229-238. DOI: 10.22052/JNS.2025.01.022

INTRODUCTION

The manganese oxide Mn_3O_4 has a normal structure with a tetragonal distortion along the C-axis, making it one of the most stable thins in the family. Mn_3O_4 possesses significant electrical and magnetic characteristics, such as metal-insulator transition materials and huge magneto resistance [1].The metal oxides are used at various technological applications such as solar cells, energy harvesting applications, catalysis, and sensors, and they are very attractive to the scientists because of their promising properties in industry [2],Among the transition metal oxides, manganese exhibits many oxidation states and therefore forms different oxides (MnO, MnO_2, Mn_2O_3, Mn_3O_4 and Mn_5O_8) [3] ,The magnetic and transport properties of these materials are closely related to their structures, crystal quality and chemical stoichiometry [4],Manganese oxide nanoparticles with various shapes and exceptional qualities have been synthesized via several innovative and novel methods [5], chemical vapor deposition [6],sol–gel [7],thermal combustion [8],pulsed laser deposition (PLD) technique [9] ,spray pyrolysis technique [10] ,Because to its high uniformity of deposit, low cost, ease of use, and low deposition temperature, spray pyrolysis was one of the most economical methods for creating manganese oxide coatings. [11]. process begins with the preparation of a precursor solution that

* *Corresponding Author Email: ly6630651@gmail.com*

contains the desired chemical components for the film. This solution is typically prepared by dissolving metal salts, organic compounds, or other precursors in a suitable solvent. The precursor solution is then atomized into fine droplets using a spray nozzle The current study aims to prepare Nano scale films of pure manganese tetragonal oxide doped with nickel oxide to study the effect of The effects of nickel oxide doping on the produced films' structural, optical and electrical characteristics Their possible usage is the reason behind this in the field of solar cell manufacturing and sensors

MATERIALS AND METHODS

Chemical spray pyrolysis (CSP) method was employed to create thin films of manganese oxide (Mn_3O_4) doped with nickel oxide (NiO). German-made glass plates from Los Las Company were prepared. The plates were cut into (2.5 × 2.5) cm dimensions and rinsed with distilled water for 4 minutes in an ultrasonic device. After that, they were sterilized with acetone for 4 minutes and then again with distilled water. Finally, they were dried with a special fabric to remove the remaining suspended particles. The oxide solution was prepared by mixing manganese chloride ($MnCl_2.4H_2O$) weighing 1.979 g in 100 ml of distilled water. Then, it was placed on a magnetic stirrer for 10 minutes. Then, it was filtered using filter paper. After that, it was deposited using a spray system on the glass plates at a temperature of 350 °C. The pure oxide films were doped with nickel oxide at ratios of (0,1, 3, 5, 7)%. Measurements have been made using a (Shimadzu XRD-6000 Powder) X-ray diffract meter with (Cu Kα) radiation within the available wavelength and range at the Technological University,and To study the effect of manganese oxide(Mn_3O_4) doping on the (NiO) films and compare the results with established values in standard cards, The spectra of transmittance and absorbance were measured using a (Shimadzu UV-Visible 1900 Spectrophotometer) Equipped with the BPC laboratory located in Baghdad Governorate, Adhamiya area.

RESULTS AND DISCUSSION

X-ray Diffraction (XRD)

The results of the diagnosis using the X-ray diffraction technique for the undoped manganese oxide Mn_3O_4 films and those doped with nickel oxide with impurity rates of (0, 1, 3, 5, 7)% showed that they have a polycrystalline structure of the tetragonal type, and The films' X-ray diffraction

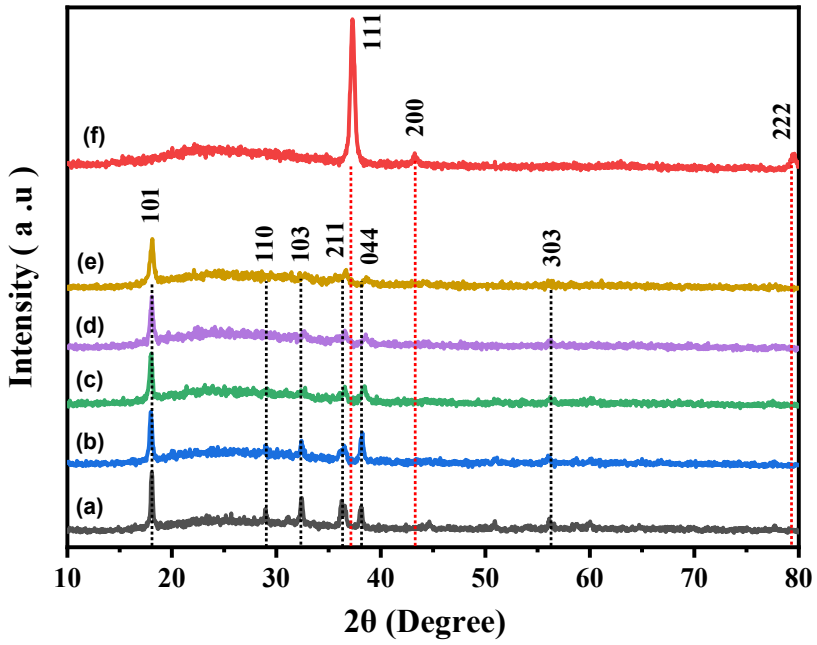

Fig. 1. X-ray diffraction patterns of (a).pure , (b).1% (c).3% , (d).5%, (e) 7% NiO -doped Mn_3O_4 thin film.

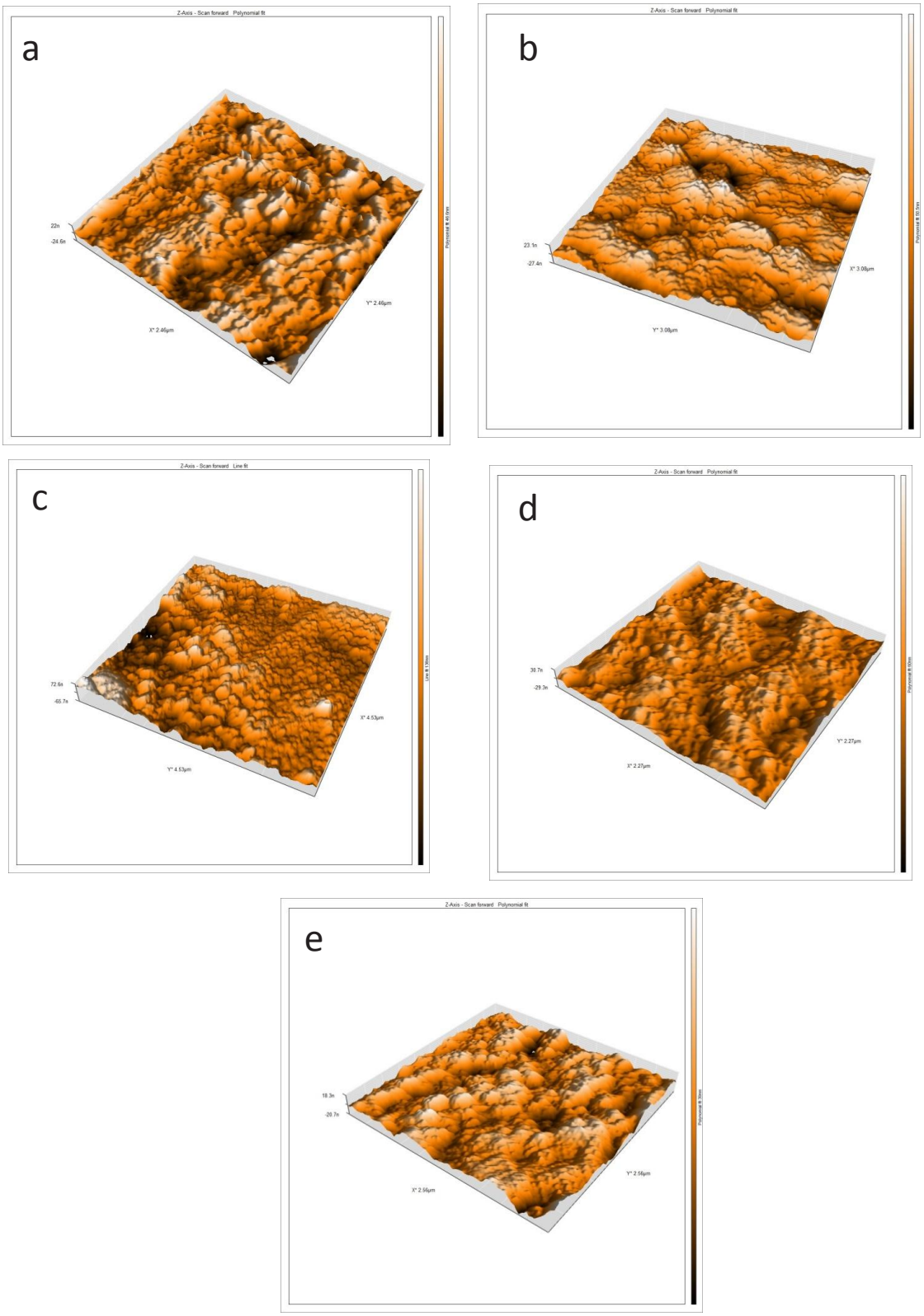

Fig. 2. a) AFM Images of pure Mn_3O_4 thin film b) AFM Images of Mn_3O_4 :NiO (1%) thin film c) AFM Images of Mn_3O_4 : NiO (3%) thin film d) AFM Images of Mn_3O_4 : NiO (5%) thin film e) AFM Images of Mn_3O_4 : NiO (7%) thin film.

patterns are displayed in Fig. 1. All prepared, by analyzing these patterns, the locations of the peaks were known We notice the appearance of levels (101,110,103,211,004,303) The prevailing trend of growth is 101 for all films, and there is no change in the prevailing trend with increasing percentages of doping with nickel oxide. It was also found that the outcomes are Most of the time, it matches the typical card with the serial no.(00-001-1127) It has been shown that doping with nickel oxide led to a change in the intensity of the peaks, especially in the dominant direction (101) in the X-ray diffraction pattern compared to the pure Mn_3O_4 film The intensity of the peak decreases and continues to decrease with increasing doping rates, and this decrease is accompanied by an increase in the width of the middle of the peak (FWHM) This means that the degree of crystallization of the films decreases with increasing doping rates. The decrease in the rate of crystallization can be described. because of the kind of link that is created between the film material's atoms, or because of the specific heat of the solid body, or resulting from the difference in the melting point in the material's constituent parts Thus, this decrease leads to the membrane material getting closer to the nano materials [12],[13] We notice that ions (NiO) were introduced into the manganese lattice (Mn_3O_4), the width of the middle of the peak increased and the intensity decreased after doping (Mn_3O_4) due to the added nickel ions, which led to a reduction in the crystalline growth of the film.This is because the ionic diameter of the nickel is (0.69 A^0) [14] smaller than the ionic diameter of manganese (0.83A^0) [15].

Results of Atomic Force Microscopy Tests (AFM)

The results (AFM) for each prepared film are depicted in Figs. 2a-e. The thin film's topography (Mn_3O_4) prepared in different proportion (1,3,5,7) % was studied using an atomic force microscope (AFM), which has a high ability to photograph and analyze the surface of thin films and also gives very accurate information about the average particle size, method of their distribution, and surface roughness values We note that the root mean square roughness (RMS) of pure (Mn_3O_4) and nickel-doped (NiO) As doping ratios increase, films shrink. The reason for this is that the films were formed with nanoparticles, where the particle size decreases with increasing doping ratios. This result is consistent with the difference in particle size obtained from XRD [16].

Optical properties

From the Fig. 3 we notice that the transmittance increases with increasing wavelength for all prepared films and continues to increase until it stabilizes at wavelengths (1100 nm). We notice

Table 1. Some topographical parameters of (Mn_3O_4 :NiO) thin films.

Sample	Average Roughness Sa (nm)	RMS (nm)	Particle Size (nm)	Surface Skewness (Ssk) (nm)	Surface Kurtosis (Sku) (nm)	Maximum Height Sz (nm)
Pure	110.7	161.7	400.4	1.234	6.940	1276
Mn_3O_4:NiO (1%)	22.93	30.08	172.1	-0.1646	3.763	239.6
Mn_3O_4:NiO (3%)	38.56	52.41	453.8	-0.05633	4.762	503.2
Mn_3O_4:NiO (5%)	30.27	38.45	134.7	0.2228	3.459	273.9
Mn_3O_4:NiO (7%)	30.00	38.14	156.8	0.9092	8.876	476.8

that the transmittance increases with increasing doping percentages and its highest value is at 3% Then the transmitted values began to decrease with increasing rates of doping with nickel oxide, and its value was lower in the pure state. The increase in transmitted values causes manganese oxide's structure to alter due to the addition of nickel electrons, which improves the quality of the crystals and crystal homogeneity, and the reduction in transmittance as nickel levels rise

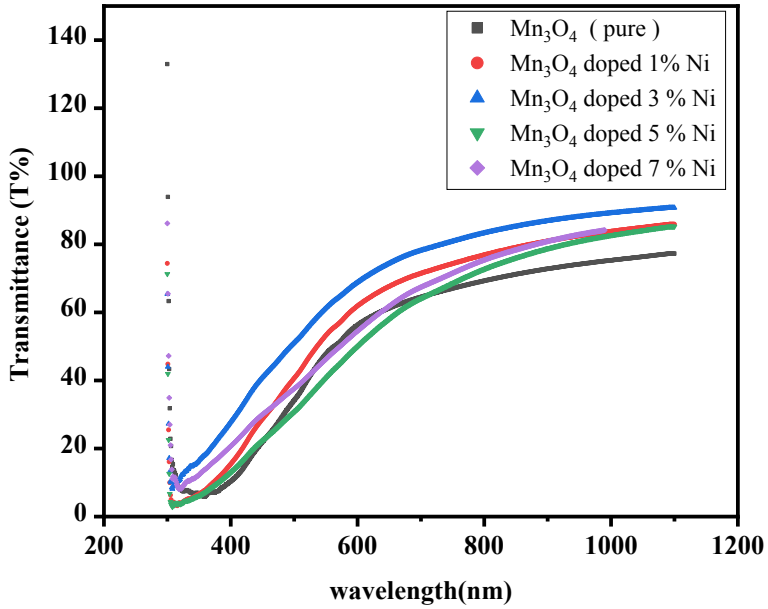

Fig. 3. Transmittance for Mn_3O_4 doping NiO films.

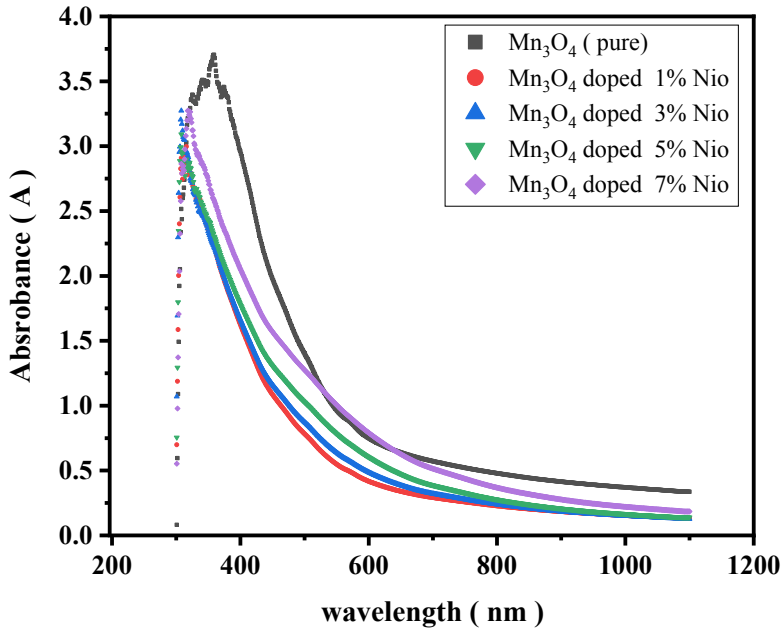

Fig. 4. Absorbance for Mn_3O_4 doping Ni O films.

concentration is due to absorption. Free carrier and ratios in granular boundaries [17] The reason for the increase in the transmittance spectrum with increasing wavelength is that the incident photons do not have sufficient energy to excite the material's electrons and thus they are transmitted. Likewise, films have a high transmittance that indicates photon absorption, and this often occurs by moving from one beam to another, and this is consistent with the results of the researcher [18]

From Fig. 4 we notice that absorbance has an opposite behavior to transmittance, as absorbance is large at short wavelengths, and as the wavelength increases, the absorbance decreases, being its lowest value at the wavelength (1100 nm) The absorbance decreases with increasing doping rates, and its lowest value is at 3% and its highest value is in the pure state. The cause is that the incident photon's energy is less than the amount of the optical energy gap of the semiconductor. Therefore, the photon cannot excite the electron and move it from the band of valence to the band of conduction,and This agrees with B.Sahin at.el [19]. We also note that there is a difference in the absorbance values of all films at each wavelength due to the homogeneity, the nature of the structure, and the difference in local levels within the energy gap due to crystalline defects, This is consistent with the researcher's results [20]

It is the ability of a material to absorb light. The absorption coefficient (α) for manganese oxide films doped with nickel oxide was calculated using the Eq. 1. Fig. 5 shows the absorption coefficient for all prepared thin films as a function of the energy of the incident photon. We notice from the results that the absorption coefficient values increase slowly at low photon energies and gradually increase more quickly with increasing incoming photon energies until they approach $\alpha \geq 10^{-4}$ cm^{-1} from the basic absorption edge region. The absorption coefficient values continue to increase For the highest incident photon energies that exceed $E_{ph} < E_g$ for all prepared films, this leads to the possibility of allowing electronic transitions between the valence and conduction bands at that energy. High values of the absorption coefficient, which are greater than 10^{-4} cm^{-1},indicate the possibility of a permissible direct transmission, while values less than 10^{-4} cm^{-1} indicate an impermissible direct transmission [21]. The behavior of the absorption coefficient changes with doping ratios and moves to the absorption edge towards higher photon energies, which leads to an increase in the energy gap values The reason for this is due to the occupation of substitution or replacement sites in the manganese oxide lattice

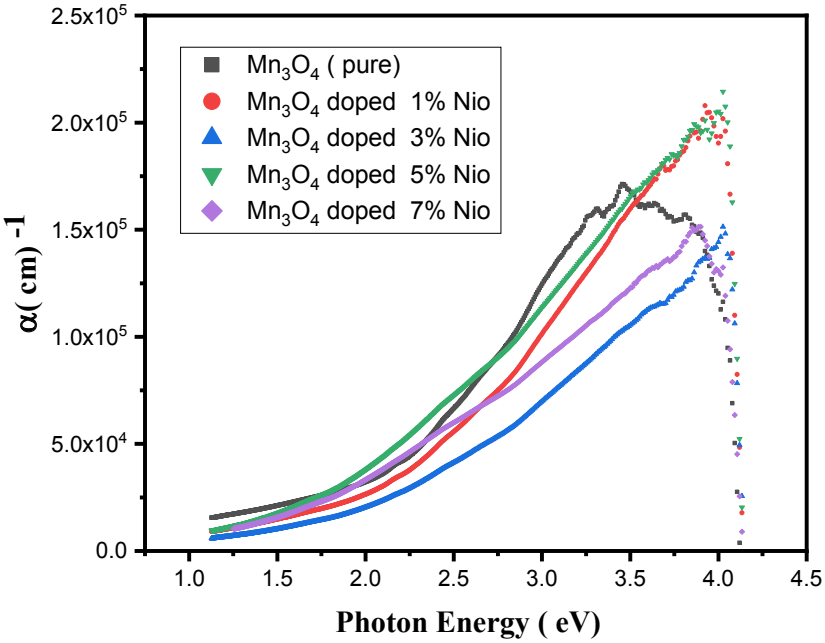

Fig. 5. Absorption Coefficient (α) for Mn_3O_4 doping Ni O films

by nickel [22].

$$\alpha = 2.303\frac{A}{t} \quad (1)$$

The crystal structure of the prepared films is the basis for determining the optical energy gap values. Using the Eq. 2 at the value of the constant r = 1/2, the values of the optical energy gap for direct transitions allowed for all prepared films

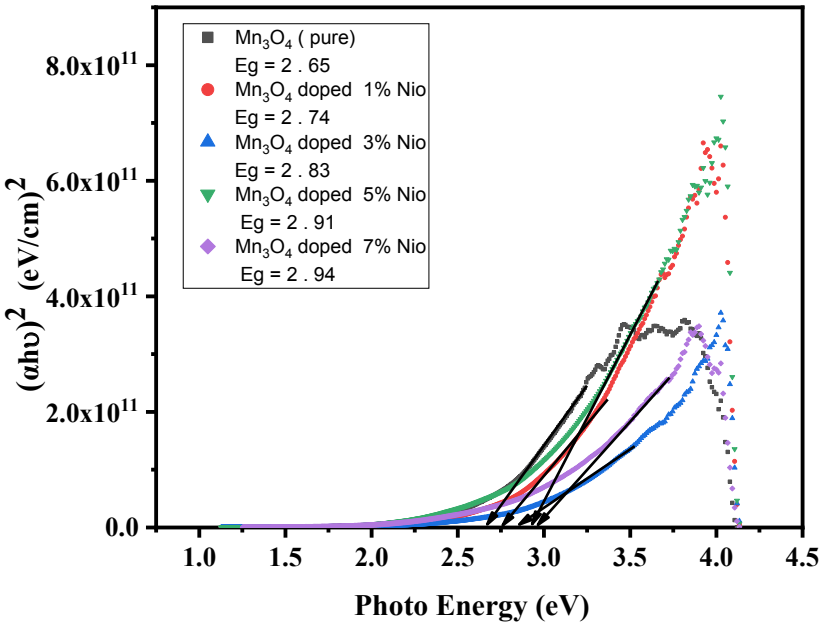

Fig. 6. Optical Energy Gap for Mn_3O_4 doping NiO films

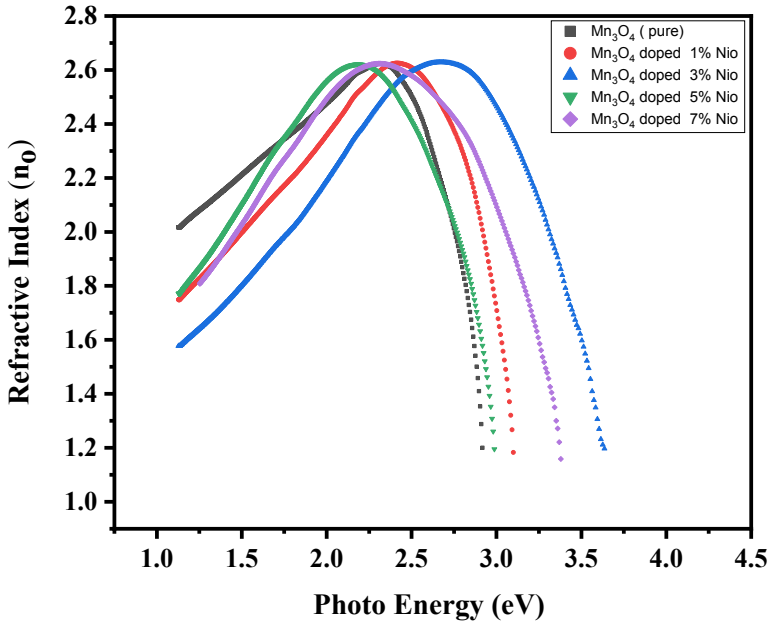

Fig. 7. Refractive Index for Mn_3O_4 doping NiO films.

were calculated. Through the graphic relationship $(\alpha h\nu)^2$ and photon energy hv,a straight line was drawn after the basic absorption edge to intersect the axis of the incident photon energy at the point $(\alpha h\nu)^2 = 0$ Thus, the intersection point represents the value of the optical energy gap of the prepared films. Fig. 6 shows the energy gap values within the range (2.65 - 2.95) eVfor the prepared films. We notice that the energy gap values change with the doping ratios of the NiO concentration, as we notice an increase in the energy gap values. The reason is that increasing the doping leads to the formation of local levels within the energy gap and near the conduction band, and thus the basic absorption edge moves to higher energy levels, and as a result, the electrons in the valence band will be displaced to a higher energy to cross these levels [23,24].

$$\alpha h\upsilon = B_1\left(h\upsilon - E_g^{'opt} \mp E_{Ph}\right)^r \qquad (2)$$

Fig. 7 shows the refractive index values as a function of the incident photon energy. For all prepared films, the refractive index values were calculated using the Eq. 3 We conclude that the refractive index values increase with increasing doping ratios for the prepared films and with increasing photon energy, and then decrease towards higher photon energy. Reflectivity and an increase in absorption coefficient values as a result of direct electronic transfer are the causes of this decline. As the concentration of a substance rises, the refractive index falls (NiO) from 1 % to 3 %,where (NiO) acts as a mediator, i.e. participates in the components of the lattice. Then the refractive index increases with an increase in the concentration of (NiO) from 3 % to 7 %,where nickel acts as a catalyst in the lattice [25].

$$n_\circ = \left[\left(\frac{1+R}{1-R}\right)^2 - (K_\circ^2 + 1)\right]^{1/2} + \frac{1+R}{1-R} \qquad (3)$$

The extinction coefficient is plotted against the incident photon's energy in Fig. 8 for all prepared films from the Eq. 4. The extinction coefficient was computed ($K_{o)}$. The figures show the similarity between the extinction coefficient curves with the absorption coefficient curves, where based on the findings, the extinction coefficient was computed.. Absorption coefficient. We note that the maximum the high photon locations are where the extinction coefficient values are found, after which the extinction coefficient values decrease

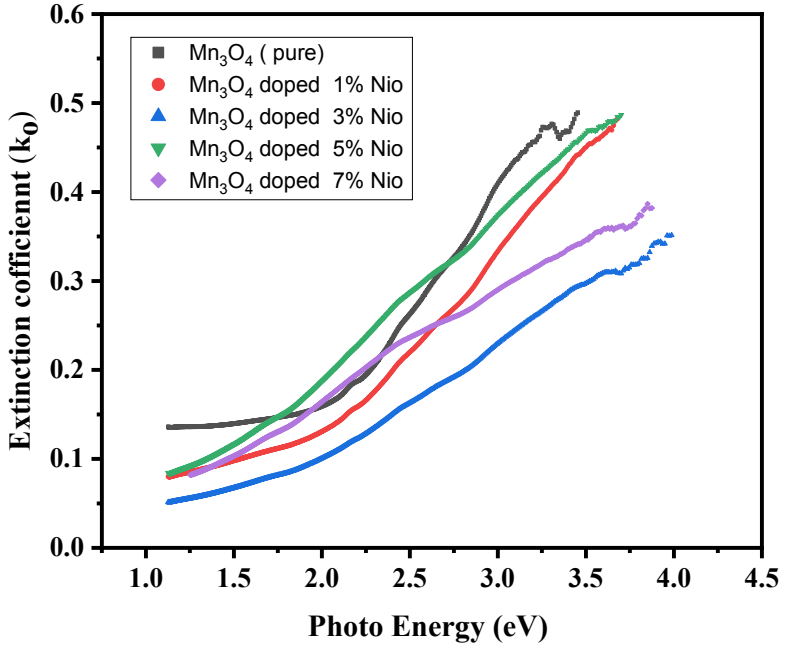

Fig. 8. Extinction Coefficient for Mn_3O_4 doping NiO films.

We notice a decrease in the extinction coefficient because the process of doping with nickel oxide leads to the donor level creation inside the energy gap, and these levels will lead to a decrease in the extinction coefficient [26,27]

$$k_\circ = \frac{\alpha\lambda}{4\pi} \quad (4)$$

CONCLUSION

The results of X-ray diffraction measurement demonstrated that the thin manganese oxide films doped with nickel oxide and prepared by chemical spray pyrolysis method have a tetragonal and polycrystalline structure and the dominant trend is (101). Through diagnosis with an atomic force microscope (AFM), it was shown that all the prepared films had a nanostructure and that root mean square values and surface roughness would both decline. It was observed through optical examinations that the transmittance of the films will rise in tandem with rising doping levels,while the absorbance decreases, and the optical energy gap, absorption coefficient, and refractive index increase with increasing photon energy. We see that when photon energy increases, the extinction coefficient values drop.

CONFLICT OF INTEREST

The authors declare that there is no conflict of interests regarding the publication of this manuscript.

REFERENCES

1. Xaba T, Shooto ND. Influence of Annealing Temperature on The Growth of Spin Coated Mn_3O_4 Thin Films From The Decomposition Of Bis(Ncyclohexyl-Salicydenaminato) Manganese(Ii) Complex. Digest Journal of Nanomaterials and Biostructures. 2021;16(1):135-142.
2. Kocyigit A. Structural, optical and electrical characterization of Mn_3O_4 thin films via Au composite. Materials Research Express. 2018;5(6):066422.
3. Jayaselvan L, Sambandam CG. Structural, optical and phase formation modifications by varying precursor temperature on Mn_2O_3 nanoparticles prepared by microwave assisted precipitation. AIP Conference Proceedings: AIP Publishing; 2020. p. 080008.
4. Ulutas C, Erken O, Gunes M, Gumus C. Effect of Annealing Temperature on The physical Properties of Mn_3O_4 Thin Film Prepared by Chemical Bath Deposition. International Journal of Electrochemical Science. 2016;11(4):2835-2845.
5. Yadav S, x S, Phogat P, Jha R, Singh S. Preparation of Tin Oxide Nanoparticles via Co-Precipitation Method for its Future Applications. International Journal of Science and Research (IJSR). 2024;13(6):1302-1306.
6. Bigiani L, Maccato C, Gasparotto A, Sada C, Barreca D. Structure and properties of Mn_3O_4 thin films grown on single crystal substrates by chemical vapor deposition. Materials Chemistry and Physics. 2019;223:591-596.
7. Kayani ZN, Nazir F, Riaz S, Naseem S. Structural, optical and magnetic properties of manganese zinc oxide thin films prepared by sol–gel dip coating method. Superlattices Microstruct. 2015;82:472-482.
8. Gosiewski K, Pawlaczyk A, Warmuzinski K, Jaschik M. A study on thermal combustion of lean methane–air mixtures: Simplified reaction mechanism and kinetic equations. Chem Eng J. 2009;154(1-3):9-16.
9. Mahmood SS, Hasan BA, Rauuf AF. Effect of Manganese Oxide Doping of Tin Oxide Thin Films on the Optical and Structural Properties. Iraqi Journal of Science. 2024:3754-3764.
10. Rossi Z, Ghannam H, Brioual B, Ullah S, Zanouni M, Diani M, et al. The tin doping effect on the physicochemical and nonlinear optical properties of the manganese oxide (Mn_3O_4: Sn) thin films. E3S Web of Conferences. 2023;469:00078.
11. Shano AM, Habeeb AA, Khodair ZT, Adnan SK. Effects of Thickness on the Structural and Optical Properties of Mn_3O_4 Nanostructure Thin Films. Journal of Physics: Conference Series. 2021;1818(1):012049.
12. Basiriparsa J, Abbasi M. High-efficiency ozone generation via electrochemical oxidation of water using Ti anode coated with Ni–Sb–SnO_2. J Solid State Electrochem. 2011;16(3):1011-1018.
13. Park S-K, Yu S-H, Pinna N, Woo S, Jang B, Chung Y-H, et al. A facile hydrazine-assisted hydrothermal method for the deposition of monodisperse SnO_2 nanoparticles onto graphene for lithium ion batteries. J Mater Chem. 2012;22(6):2520-2525.
14. Karpagavalli S, Vethanathan SJK, Perumal S. Effect of nickel doping on the structural, optical, electrochemical and magnetic properties of hausmannite (Mn_3O_4) nanoparticles. International Journal of Nanoparticles. 2019;11(4):305.
15. Jha A, Thapa R, Chattopadhyay KK. Structural transformation from Mn_3O_4 nanorods to nanoparticles and band gap tuning via Zn doping. Mater Res Bull. 2012;47(3):813-819.
16. Larbi T, Haj Lakhdar M, Amara A, Ouni B, Boukhachem A, Mater A, et al. Nickel content effect on the microstructural, optical and electrical properties of p-type Mn_3O_4 sprayed thin films. J Alloys Compd. 2015;626:93-101.
17. Dagdelen F, Serbetci Z, Gupta RK, Yakuphanoglu F. Preparation of nanostructured Bi-doped CdO thin films by sol–gel spin coating method. Mater Lett. 2012;80:127-130.
18. Moreno R, Ramirez EA, Gordillo Guzmán G. Study of optical and structural properties of CZTS thin films grown by co-evaporation and spray pyrolysis. Journal of Physics: Conference Series. 2016;687:012041.
19. Şahin B, Taşköprü T, Bayansal F. Bandgap variation of nanostructure tin doped CdO films via SILAR processing. Ceram Int. 2014;40(6):8709-8714.
20. Prabhakar RR, Zhenghua S, Xin Z, Baikie T, Woei LS, Shukla S, et al. Photovoltaic effect in earth abundant solution processed Cu2MnSnS4 and Cu2MnSn(S,Se)4 thin films. Sol Energy Mater Sol Cells. 2016;157:867-873.
21. Mullerova J, Sutta P. On Some Ambiguities of the Absorption Edge and Optical Band Gaps of Amorphous and Polycrystalline Semiconductors. Communications - Scientific letters of the University of Zilina. 2017;19(3):9-15.

22. Nallendran R, Selvan G, Balu AR. NiO coupled CdO nanoparticles with enhanced magnetic and antifungal properties. Surfaces and Interfaces. 2019;15:11-18.
23. Guia LM, Sallet V, Hassani S, Martínez-Tomás MC, Muñoz-Sanjosé V. Effect of Growth Temperature on the Structural and Morphological Properties of MgCdO Thin Films Grown by Metal Organic Chemical Vapor Deposition. Crystal Growth & Design. 2017;17(12):6303-6310.
24. Hammoodi FG, Shuihab AA, Ebrahiem SA. Synthesis and studying of some properties of CdO:in thin films. AIP Conference Proceedings: AIP Publishing; 2022. p. 090032.
25. El-Ghany HAA. Physical and Optical Characterization of Manganese Ions in Sodium-Zinc -Phosphate Glass Matrix. IARJSET. 2018;5(12):43-53.
26. Hassouni MH, Mishjil KA, Chiad SS, Habubi NF. Effect of Gamma Irradiation on the Optical Properties of Mg Doped CdO Thin Films Deposited by Spray Pyrolysis. International Letters of Chemistry, Physics and Astronomy. 2013;16:26-37.
27. Structural and Optical Properties of Sno2:Mno2 Nanostructure Thin Films. Nanotechnology Perceptions. 2024.